A maize wall-associated kinase confers quantitative resistance to head smut

Weiliang Zuo[1,5], Qing Chao[1,5], Nan Zhang[1,5], Jianrong Ye[1], Guoqing Tan[2], Bailin Li[3], Yuexian Xing[2], Boqi Zhang[1], Haijun Liu[4], Kevin A Fengler[3], Jing Zhao[1], Xianrong Zhao[1], Yongsheng Chen[1], Jinsheng Lai[1], Jianbing Yan[4] & Mingliang Xu[1]

Head smut is a systemic disease in maize caused by the soil-borne fungus *Sporisorium reilianum* that poses a grave threat to maize production worldwide. A major head smut quantitative resistance locus, *qHSR1*, has been detected on maize chromosome bin2.09. Here we report the map-based cloning of *qHSR1* and the molecular mechanism of *qHSR1*-mediated resistance. Sequential fine mapping and transgenic complementation demonstrated that *ZmWAK* is the gene within *qHSR1* conferring quantitative resistance to maize head smut. ZmWAK spans the plasma membrane, potentially serving as a receptor-like kinase to perceive and transduce extracellular signals. *ZmWAK* was highly expressed in the mesocotyl of seedlings where it arrested biotrophic growth of the endophytic *S. reilianum*. Impaired expression in the mesocotyl compromised *ZmWAK*-mediated resistance. Deletion of the *ZmWAK* locus appears to have occurred after domestication and spread among maize germplasm, and the ZmWAK kinase domain underwent functional constraints during maize evolution.

Maize (*Zea mays* L.) is the most widely grown crop worldwide and is a central food and forage staple as well as an important source of biofuel and other industrial materials. By the 2050s, the human population is predicted to reach 9.2 billion (see URLs). To feed this huge population, it will be necessary not only to improve the yield potential of major crops but also to reduce yield losses from biotic and abiotic factors.

Head smut is a systemic fungal disease caused by *S. reilianum* that occurs in most maize-growing areas (see URLs) and causes tremendous loss of yield during outbreaks[1]. The soil-borne pathogen *S. reilianum* invades the maize seedling and grows vegetatively until it reaches the flower primordia, where it then switches to reproductive sporulation, which leads to massive black sori in the inflorescences, referred to as head smut (**Fig. 1a,b**). *S. reilianum* infection can also cause phyllody of the ear and tassel and/or stunted growth[2]. Head smut disease results in complete yield loss for infected plants, and the most economical and environmentally friendly method to reduce yield losses is to breed and deploy resistant maize hybrids.

In comparison with other cereal crops, such as rice (*Oryza sativa*) and wheat (*Triticum aestivum*), maize has fewer qualitative resistance genes that have been extensively used by breeders[3]. Only three of these—*Hm1* (conferring resistance to *Cochliobolus carbonum* race 1), *Rp1-D* (conferring resistance to common rust, *Puccinia sorghi*) and *Rxo1* (conferring resistance to rice bacterial streak disease)—have been resolved to the causative genes[4–6]. Instead, maize has relatively more quantitative resistance loci deployed in the field to counter the

majority of diseases[7]. The cumulative effects of multiple smaller-effect quantitative resistance loci can produce high or even complete resistance[8,9]. Moreover, quantitative resistance is usually more durable than qualitative resistance[10,11]. However, map-based cloning of resistance-conferring quantitative trait loci (QTLs) has proven extremely difficult, owing to (i) small genetic effects, (ii) variations in disease severity across different geographical locations and years, and (iii) lack of uniformity in the evaluation of disease symptoms[12–15]. Thus far, only one resistance QTL in maize, *Rcg1*, which confers resistance against anthracnose stalk rot, has been resolved to the causal variants[16]. Here we report the map-based cloning of *qHSR1*, a major head-smut resistance QTL, and explore the molecular mechanism associated with resistance.

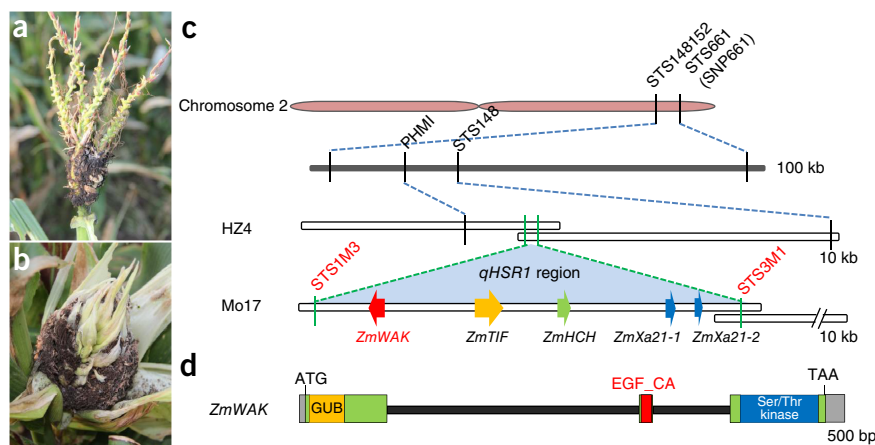## RESULTS

Fine mapping of *qHSR1*

We previously detected a dominant QTL, *qHSR1*, on the long arm of chromosome 2, which could reduce head smut disease incidence by ~25% (ref. 17). This QTL has consistently been detected in various mapping populations[18,19]. Introduction of *qHSR1* into head smut–susceptible lines via marker-assisted selection can significantly reduce disease incidence across years, demonstrating the great potential of *qHSR1* in the genetic control of head smut disease in maize[20].

To fine map *qHSR1*, we generated multigenerational backcross populations of Ji1037 (highly resistant) and Huangzoa4 (HZ4; highly susceptible) and developed high-density molecular markers in the

Figure 1 Fine mapping of the resistance QTL *qHSR1*. (**a**,**b**) Head smut symptoms in the tassel (**a**) and ear (**b**). (**c**) Sequential fine mapping of *qHSR1*. The vertical lines represent the sites of key molecular markers, and the two green vertical lines indicate the flanking markers STS1M3 and STS3M1 in the final mapping step. The HZ4 and Mo17 BAC contigs are represented by overlapping unfilled rectangles, and the predicted genes *ZmWAK*, *ZmTIF*, *ZmHCH*, *ZmXa21-1* and *ZmXa21-2* are depicted by colored arrows. (**d**) Gene structure of *ZmWAK*. Gray boxes represent the 3′ and 5′ UTRs, and the positions of the coding regions for the GUB, EGF_CA and kinase domains are indicated.

qHSR1 region (**Supplementary Table 1**). By using a recombinant-derived progeny testing strategy[21], we successively obtained 140 recombinants and ultimately narrowed *qHSR1* to an interval flanked by the markers STS1M3 and STS3M1 (**Supplementary Fig. 1a–c**). Consistent with the QTL analysis, *qHSR1* reduced head smut incidence by 18.6–26.7% across multiple backcross generations (**Supplementary Fig. 1d**).

ZmWAK is the candidate resistance gene

The *qHSR1*-tagged markers STS1M3 and STS3M1 were used to screen Mo17 (with the same *qHSR1* region as Ji1037) and HZ4 BAC libraries. *qHSR1*-containing BAC clones were sequenced and annotated (**Fig. 1c**). Interestingly, the *qHSR1* region flanked by markers STS1M3 and STS3M1 varied substantially in length between the maize lines. The Mo17 interval was 152 kb, whereas the HZ4 interval was only 5 kb (**Fig. 1c**). This 147-kb deletion in HZ4 could explain why we did not obtain recombinants within the STS1M3–STS3M1 interval in this line.

Moreover, we selected several key recombinants to generate four inter-cross populations. The individuals with the 152-kb DNA segment had disease incidence that was reduced by ~20%, thereby confirming the presence of *qHSR1* in the 152-kb region (**Supplementary Fig. 2**).

There were five annotated genes in the 152-kb interval of *qHSR1* from Mo17: *ZmWAK*, *ZmHCH*, *ZmTIF*, *ZmXa21-1* and *ZmXa21-2* (**Fig. 1c,d**). We aligned the predicted Mo17 genes with the corresponding genome sequence from B73 (a moderately resistant inbred line; ~5% diseased plants in the field), which showed that *ZmXa21-1* and *ZmXa21-2* were completely missing in B73, whereas *ZmHCH* and *ZmTIF* had pronounced structural differences and only *ZmWAK* was intact (**Supplementary Fig. 3**). An RNA expression assay demonstrated that *ZmWAK* was expressed in all tissues of Ji1037 seedlings, whereas *ZmHCH* and *ZmXa21-1* were specifically expressed in root and coleoptile, respectively. *ZmTIF* and *ZmXa21-2* were not expressed in any of the tissues examined (**Supplementary Fig. 4**). Furthermore, we developed markers for each of the expressed
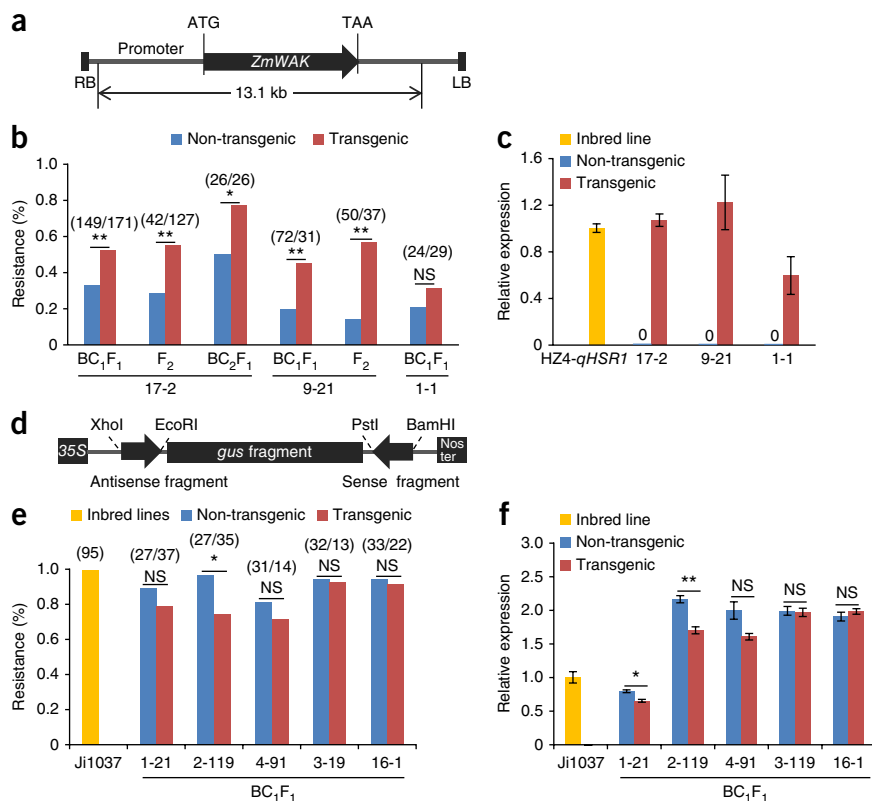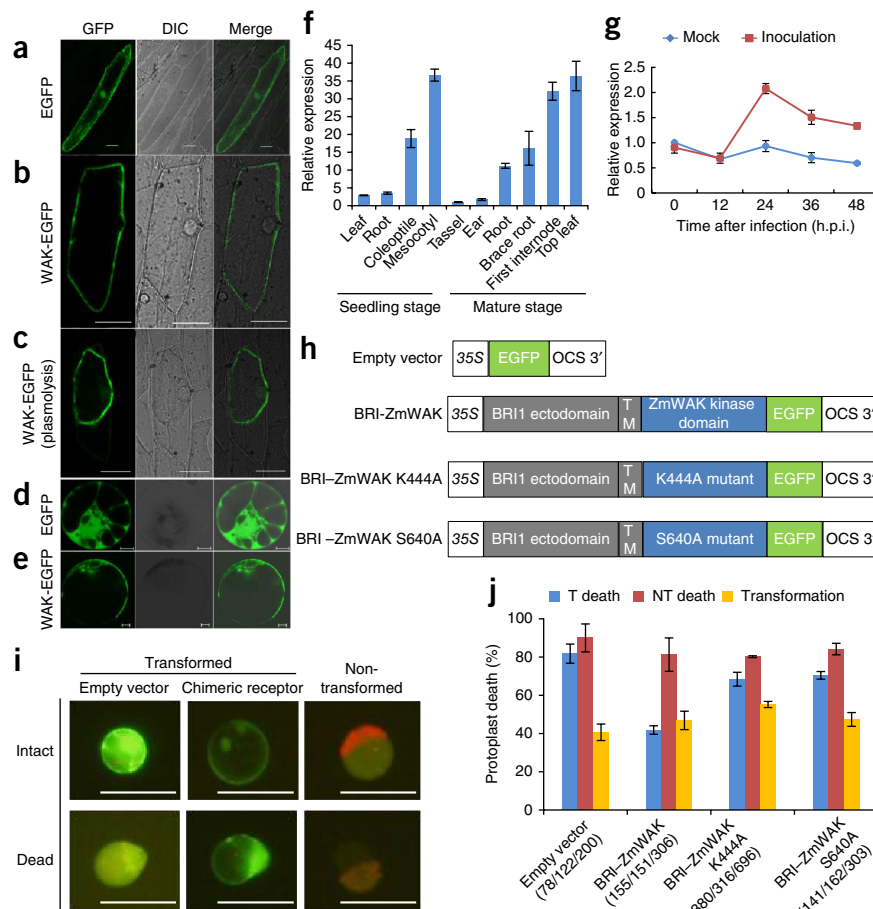

Figure 2 Transgenic validation of *ZmWAK*. (**a**) Structure of pCAMBIA1300-ZmWAK used for the complementation assay. The construct contains the entire *ZmWAK* gene and the 3.9-kb promoter region. LB, left border; RB, right border. (**b**) The resistance performance of pCAMBIA1300-ZmWAK–transformed transgenic plants. The sample size of each group is indicated in parentheses. (**c**) The relative expression levels of *ZmWAK* in the mesocotyl of F_2 progeny from three complementary transgenic events. The data were normalized to the sample of HZ4-*qHSR1*. Expression values are means ± s.d. Each sample contained five individuals. There was no expression in non-transgenic plants. (**d**) Schematic of the RNAi construct pGreen-WAK. Nos ter, Nos terminator. (**e**) Resistance performance of *ZmWAK* RNAi transgenic plants. The sample size of each group is indicated in parentheses. (**f**) The relative expression levels of *ZmWAK* in mesocotyl for five RNAi transgenic events. Data were normalized to the sample of Ji1037. Expression values are means ± s.d. Each sample contained five individuals. A χ^2 test of independence or a Fisher's exact test indicated a significant difference. **$P < 0.01$, *$P < 0.05$; NS, not significant.

Figure 3 Subcellular localization and expression pattern of ZmWAK. (**a–e**) Confocal scanning (GFP; left), differential interference contrast (DIC; middle) and merged (right) micrographs of onion epidermal cells transformed with the pEZS-NL vector (**a**) or the 35S::WAK-EGFP construct and left untreated (**b**) or subjected to plasmolysis (**c**). Scale bars, 50 μm. (**d,e**) Maize protoplasts transformed with the pEZS-NL vector (**d**) or the 35S::WAK-EGFP construct (**e**). Scale bars, 5 μm. (**f**) Expression of ZmWAK in different tissues of Ji1037 plants. Values are the means ± s.d. of three independent experiments with five individuals per sample. Data were normalized to the tassel sample. (**g**) Expression of ZmWAK in Ji1037 after inoculation with S. reilianum. Data were normalized to the mock-inoculation sample at 0 hours post-inoculation (h.p.i.). Values are the mean ± s.d. from three biological replications with ten individuals per sample. (**h**) Schematic of the expression constructs for the chimeric receptor (BRI-ZmWAK) and chimeric receptor with a mutated kinase domain (BRI-ZmWAKm). Gray rectangles indicate the ectodomain of BRI1, and blue rectangles indicate the cytoplasmic domain of ZmWAK. The coding sequence for the chimeric receptor was expressed under the 35S promoter and fused with the coding sequence for an EGFP tag to detect transformed cells. The mutated amino acids are shown. TM, transmembrane region; OCS, octopine synthase terminator. (**i**) Micrographs of intact and dead cells in the empty vector– and chimeric receptor–transformed and non-transformed (red auto-fluorescence) groups. Scale bars, 50 μm. (**j**) Death rates of protoplasts expressing empty vector, BRI-ZmWAK, BRI–ZmWAK K444A or BRI–ZmWAK S640A after brassinolide treatment. T, transformed; NT, non-transformed. Values are the mean ± s.d. of two independent experiments. The sample sizes of each group are indicated in parentheses.

genes (**Supplementary Fig. 5a**) and investigated the presence/absence of variation (PAV) within a panel of 62 diverse maize inbred lines, which were either resistant or highly susceptible to head smut. We found that ZmWAK and ZmHCH were present in all resistant and some susceptible lines, whereas ZmXa21-1 was randomly detected in both resistant and susceptible inbred lines (**Supplementary Fig. 5b**). Taken together, these findings suggested that ZmWAK is very likely the gene responsible for the head smut resistance attributed to qHSR1.

To validate our hypothesis that ZmWAK confers resistance to head smut, we isolated a 13.1-kb genomic fragment from a Mo17 BAC clone, containing the intact coding and 3.92-kb promoter regions of ZmWAK. Three independent transgenic events were obtained by introducing the exogenous ZmWAK into the maize hybrid Hi-II (**Fig. 2a**). We crossed the transgenic T_1 plants to HZ4 (lacking ZmWAK) to produce an F_1 population. The transgenic F_1 plants were either selfed or backcrossed to HZ4 to produce F_2, BC_1F_1 and BC_2F_1 populations for functional complementation tests. In the BC_1F_1 and BC_2F_1 populations (except for the BC_1F_1 population of event 1-1), the disease incidence of transgenic plants was significantly reduced (by 19.2–26.9%; $P < 0.05$) in comparison to the resistance of their non-transgenic sibling lines. In the F_2 population, the disease incidence of transgenic plants, consisting of both homozygotes and heterozygotes for exogenous ZmWAK, was reduced by 26.5–42.8% (**Fig. 2b**). Correspondingly, transgenic plants from events 17-2 and 9-21 had comparable expression levels of ZmWAK to those observed in HZ4-qHSR1
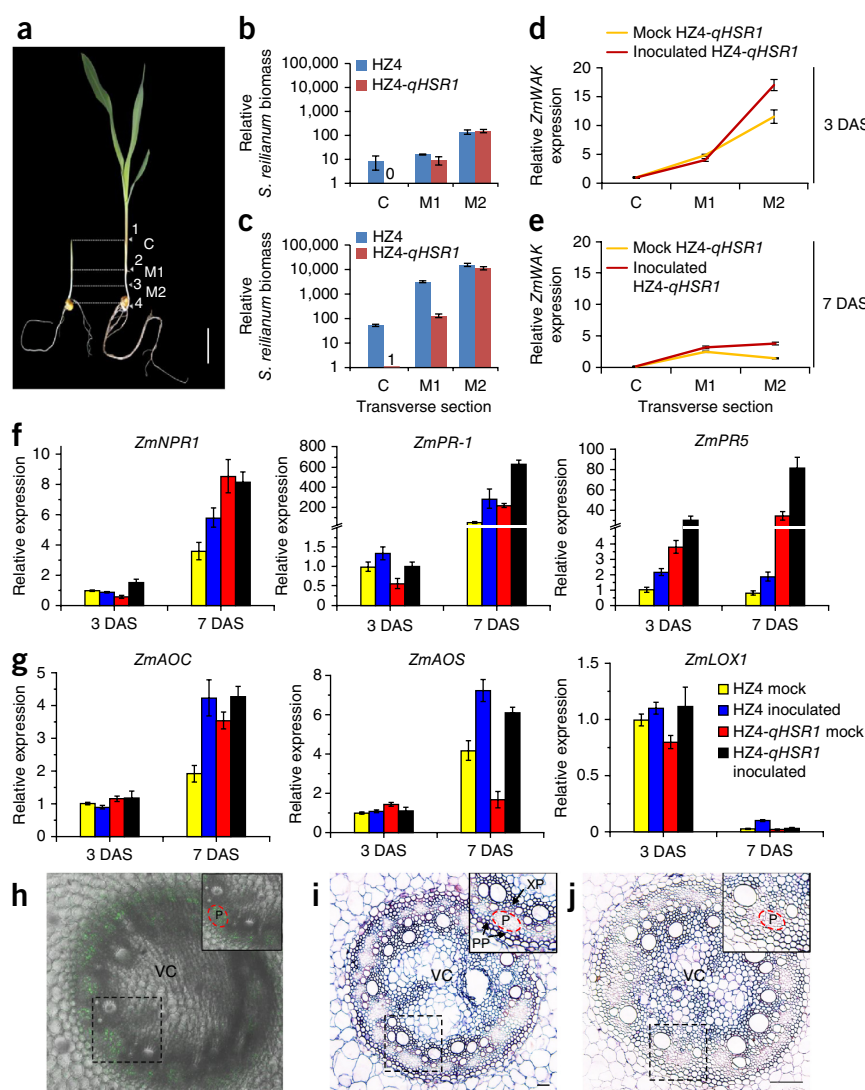
(an HZ4 near-isogenic line with the resistance QTL), whereas transgenic plants from event 1-1 showed significantly low expression levels (**Fig. 2c**). Furthermore, we transformed Hi-II with a ZmWAK RNA interference (RNAi) construct (**Fig. 2d**), and the transgenic T_1 plants were crossed with Ji1037 twice to produce BC_1F_1 populations. All transgenic BC_1F_1 plants from five independent events showed reduced resistance to head smut relative to the non-transgenic controls, although only one event (2-119) resulted in a significant reduction ($P < 0.05$; **Fig. 2e**). Impaired resistance was associated with RNAi-mediated knockdown of ZmWAK (**Fig. 2f**). Apart from event 1-21, the other four transgenic events resulted in enhanced expression levels of ZmWAK in comparison to Ji1037, and this presumably resulted from hybrid vigor. All these results indicate that ZmWAK is the gene in qHSR1 responsible for head smut resistance.

Characterization of ZmWAK

We obtained the complete transcript sequence of ZmWAK by RACE using RNA isolated from Ji1037 seedling roots. ZmWAK encodes a 730-residue receptor-like protein with domain characteristics of the wall-associated kinase (WAK) family, including a cytoplasmic serine/threonine kinase domain, a calcium-binding epidermal growth factor (EGF_CA) domain and an extracellular galacturonan-binding (GUB) domain (**Fig. 1d** and **Supplementary Fig. 6a**). WAKs constitute a large family of proteins that participate in many aspects of plant life. In *Arabidopsis thaliana*, WAK and WAK-like proteins are involved in various signaling pathways, including disease resistance[22,23],

Figure 4 ZmWAK functions in mesocotyl to inhibit the upward growth of *S. reilianum*. (**a**) Maize seedlings at 3 (left) and 7 (right) DAS, with numbered arrowheads indicating the borders of the different sections: 1, coleoptilar tip; 2, coleoptilar node; 3, midpoint of the mesocotyl; 4, joint between the mesocotyl and seed. These borders delineated the three transverse sections sampled: the whole coleoptile (C), the upper half of the mesocotyl (M1) and the lower half of the mesocotyl (M2). Scale bar, 3 cm. (**b,c**) Quantification of *S. reilianum* in the three sections by quantitative PCR (qPCR) at 3 (**b**) and 7 (**c**) DAS. Data were normalized to the sample of HZ4-*qHSR1* coleoptile at 7 DAS. (**d,e**) The expression patterns of *ZmWAK* in the three sections of HZ4-*qHSR1* at 3 (**d**) and 7 (**e**) DAS. Data were normalized to the sample of mock-inoculated HZ4-*qHSR1* at 3 DAS. (**f,g**) Expression of the salicylic acid–responsive resistance genes *ZmNPR1*, *ZmPR-1* and *ZmPR5* (**f**) and the jasmonate-responsive genes *ZmAOC*, *ZmAOS* and *ZmLOX1* (**g**) in the lower mesocotyl of HZ4 and HZ4-*qHSR1* seedlings after *S. reilianum* inoculation. Data were normalized to the sample of mock-inoculated HZ4 at 3 DAS. Each value in **b**–**g** represents the mean ± s.d. from three biological replications; each sample was collected from at least ten individuals. (**h**) Massive dot signals of *S. reilianum* in the transverse section of mesocotyl at 7 DAS visualized with wheat germ agglutinin (WGA)–Alexa Fluor 488. Scale bar, 100 μm. (**i,j**) *ZmWAK* RNA *in situ* hybridization in 8-μm transverse sections from the mesocotyl of HZ4-*qHSR1* plants at 7 DAS: hybridization signals with the antisense (**i**) and sense (**j**) probe. Scale bars, 20 μm (**i**) and 50 μm (**j**). VC, vascular cylinder; XP, xylem parenchyma; PP, pericycle parenchyma; P, phloem. The red circle indicates the phloem. The dashed rectangle was annotated at the top right.

heavy-metal (aluminum) tolerance[24] and development[25–27]. In cereals, the WAK family expanded during evolution to produce members with different tissue-specific, developmentally controlled and external stimuli–induced expression patterns[28,29]. Maize has >100 annotated *WAK* genes distributed across multiple chromosomes. On the basis of the presence or absence of arginine (R) adjacent to the catalytic aspartate (D), WAKs can be classified into RD and non-RD kinases. Unlike its *Arabidopsis* orthologs (encoding RD kinases), *ZmWAK* encodes a non-RD kinase (**Supplementary Fig. 6a**). Most pattern-recognition receptors (PRRs) that recognize conserved microbial or pathogen-associated molecular patterns are non-RD kinases[30]. In phylogenetic analysis, RD and non-RD ZmWAK kinases in maize with complete versions of all three domains (GUB, EGF_CA and kinase) tended to separately cluster in different clades, suggesting their functional divergence (**Supplementary Fig. 6b**).

We examined the subcellular localization of ZmWAK following transient expression of a ZmWAK–enhanced green fluorescent protein (EGFP) fusion construct in both onion epidermal cells and maize protoplasts. We found that ZmWAK was localized to the plasma membrane before and after plasmolysis (**Fig. 3a**–**e**), consistent with its predicted role as an extracellular signal receptor. We also examined basal *ZmWAK* expression in various tissues of Ji1037 seedlings and

adult plants (before heading), finding expression to varying degrees in different tissues. In seedlings, for instance, *ZmWAK* expression in the mesocotyl was ~10-fold higher than its expression in leaves or roots, whereas in adult plants *ZmWAK* was mainly expressed in the first above-ground internode and top leaf (**Fig. 3f**). Additionally, *ZmWAK* expression was induced in the coleoptile 12 h after plants were challenged with mixed mating–compatible sporidia of *S. reilianum* (**Fig. 3g**).

In *Arabidopsis*, the AtWAK1 receptor perceives oligogalacturonides, a degraded product of the plant cell wall[31], and AtWAK2 is involved in perceiving pectin and in turgor maintenance[32,33]. Given that ZmWAK shows high sequence similarity to AtWAK2, we hypothesized that ZmWAK might have a similar role in osmotic regulation. We thus constructed a chimeric receptor composed of the cytoplasmic ZmWAK kinase domain and the ectodomain of *Arabidopsis* brassinosteroid insensitive 1 (BRI1) (**Fig. 3h**). We introduced the construct into maize protoplasts to determine whether the chimeric receptor could perceive the extracellular brassinolide signal to induce intracellular WAK kinase signaling and adjust the osmatic pressure. Treatment with brassinolide caused cell death (**Fig. 3i**) in up to 81.5% of the cells transformed with the empty vector, a result not significantly different from that in non-transformed cells (89.7% cell death). By contrast,

Table 1 PAV polymorphism of *ZmWAK*

	Group	Total	Presence	Absence	Absence/total (%)
Maize	Mixed	112	92	20	17.9
	NSS	136	115	21	15.4
	SS	32	31	1	3.1
	TST	223	175	48	21.5
	Total	503*	413	90	17.9
Teosinte	NA	184	184	0	0.7

The *ZmWAK* deletion was observed in maize but not in teosinte. An asterisk indicates 503 lines from 522 maize lines having population information. NA, not available.

a much lower proportion of cells expressing the chimeric BRI-ZmWAK construct died after treatment (41.7%). When expressing the kinase-mutated chimeric constructs BRI–ZmWAK Lys44Ala (an ATP-binding site mutant) or BRI–ZmWAK Ser640Ala (a predicted phosphorylation site mutant) (**Fig. 3h**), maize protoplasts were weakly protected from osmotic stress in comparison to protoplasts expressing BRI-ZmWAK, as indicated by the fact that the percentages of dead cells became much closer in the transformed and non-transformed cells (**Fig. 3j**). These findings indicate that the ability of ZmWAK to transduce extracellular signals is dependent on its kinase activity and suggest that ZmWAK participates in the maintenance of turgor in maize, although it is not yet clear how these functions contribute to disease resistance.

ZmWAK arrests *S. reilianum* in mesocotyl

S. reilianum teliospores overwinter in soil and invade maize seedlings through the root after seed emergence[34]. The development of smut on ears or tassels depends largely on whether the fungus reaches the shoot meristem[35]. The mesocotyl connects the base of the coleoptile and the seed; hence, *S. reilianum* needs to pass through the mesocotyl to penetrate the apical meristem for successful infection. Given that *ZmWAK* is highly expressed in mesocotyl (**Fig. 3f**), we speculated that the mesocotyl might be the main area for maize defense against *S. reilianum* invasion.

To address this possibility, we investigated in detail three transverse sections from maize seedlings, including the coleoptile, the upper half of the mesocotyl and the lower half of the mesocotyl (**Fig. 4a**). At 3 days after sowing (DAS), the coleoptile had emerged from the soil surface, and mesocotyl elongation had stopped; *S. reilianum* showed a gradient of distribution in HZ4 plants (without *ZmWAK*), from high abundance in the lower mesocotyl to low abundance in the coleoptile. In comparison to the parental HZ4 line, the near-isogenic line HZ4-*qHSR1* had similar amounts of *S. reilianum* in the upper and lower mesocotyl and no detectable fungal mycelia in the coleoptile (**Fig. 4b**). At 7 DAS, the amount of *S. reilianum* increased dramatically in all three sections in HZ4 seedlings, whereas HZ4-*qHSR1* seedlings showed similarly high *S. reilianum* levels in the lower mesocotyl but much lower levels in the upper mesocotyl (only about 4% of those in HZ4) and slightly detectable amounts in the coleoptile (**Fig. 4c**). *ZmWAK* also showed a gradient of expression in HZ4-*qHSR1* at 3 DAS, from very high in mesocotyl to relatively low in coleoptile (**Fig. 4d**). However, *ZmWAK* expression decreased in all sections at 7 DAS, especially in the lower mesocotyl (**Fig. 4e**). *ZmWAK* was responsive to *S. reilianum* challenge, as *ZmWAK* expression was increased in mesocotyl at 3 DAS (**Fig. 4d**) and 7 DAS (**Fig. 4e**) in comparison to non-inoculated plants.

We also examined the expression of salicylic acid– and jasmonate-responsive genes[36]. The basal expression levels of salicylic acid–responsive genes in HZ4-*qHSR1* were comparable to those in HZ4 for *ZmPR5*

or significantly ($P < 0.05$) lower than those in HZ4 for *ZmNPR1* and *ZmPR-1* at 3 DAS. However, all three genes in HZ4-*qHSR1* had expression levels higher than those in HZ4 at 7 DAS. When we challenged seedlings with *S. reilianum*, *ZmPR-1* and *ZmPR5* levels were upregulated in both HZ4-*qHSR1* and HZ4; moreover, HZ4-*qHSR1* showed respective 2.6- and 2.3-fold higher expression for *ZmPR-1* and *ZmPR5* than HZ4 at 7 DAS. By contrast, the expression of *ZmNPR1* was only induced in HZ4-*qHSR1* at 3 DAS and in HZ4 at 7 DAS (**Fig. 4f**). In comparison to the salicylic acid–responsive genes, the jasmonate-responsive genes were also induced in both HZ4 and HZ4-*qHSR1* at 3 (Zm*LOX1*) and 7 (Zm*AOC* and Zm*AOS*) DAS but showed a slight difference between the two lines (**Fig. 4g**). The induced expression of jasmonate-responsive genes in both HZ4 and HZ4-*qHSR1* might be associated with the pathogenic activity of *S. reilianum*, as reported in the *Ustilago*-maize pathosystem[37].

In mesocotyl, *S. reilianum* mainly colonized and accumulated in the phloem (**Fig. 4h**). Intriguingly, *ZmWAK* expression was almost undetectable inside the phloem by RNA *in situ* hybridization. By contrast, *ZmWAK* was highly expressed in the xylem parenchyma cells and pericycle parenchyma cells encircling the phloem (**Fig. 4i,j**). Taken together, these results suggest that ZmWAK might 'monitor' the activity of *S. reilianum* and induce innate immunity to inhibit the biotrophic growth of *S. reilianum* from reaching aerial tissues, thus reducing disease incidence.

Impaired *ZmWAK* expression compromises resistance

Introgression of the *qHSR1* region of the Ji1037 line into ten susceptible lines via marker-assisted selection greatly improves head smut resistance[20]. We investigated the PAV at the *ZmWAK* locus for these ten susceptible lines and found that only five of them (8902, 8903, 982, V022 and V4) contained *ZmWAK*. To investigate whether allelic variation at the sequence level or an expression difference was responsible for the variation in resistance among the lines, we sequenced *ZmWAK* for the highly susceptible lines 8902, 982, V022 and V4, the moderately resistant line B73 and the resistant line Zheng58. Comparing the translated ZmWAK protein sequences to that of Ji1037, we detected amino acid changes at eight sites, including seven substitutions and one deletion (**Supplementary Fig. 7a,b**). However, Protein Variation Effect Analyzer (PROVEAN) software predicted that none of the substitutions or the deletion would have deleterious effects on ZmWAK function (**Supplementary Fig. 7c**). In contrast, we detected significant differences ($P < 0.05$) in *ZmWAK* expression in mesocotyl among the different lines but not in roots or leaves (**Supplementary Fig. 7d**). These results suggest that the susceptibility of some maize lines is primarily due to their relatively low levels of *ZmWAK* expression in mesocotyl rather than to amino acid changes in the encoded protein.

Evolutionary aspects of the *ZmWAK* locus

Maize has relatively high genomic diversity in comparison to other crops[38]. In addition to SNPs, copy number variation and PAV are common and widely distributed in the maize genome, and these structural variations are thought to be related to quantitative traits[39,40]. In the *qHSR1* region, the susceptible line HZ4 had a 147-kb deletion, and there was high gene PAV in the panel of 62 diverse inbred lines (**Supplementary Fig. 5b**). We thus expanded our investigation of *ZmWAK* PAV to include another 522 maize inbred lines[41] and 184 teosinte accessions (*Zea* spp.) to examine the origin and distribution of *ZmWAK*. The *ZmWAK* deletion was only present in maize germplasm and not in the teosinte accessions we examined (**Table 1** and **Supplementary Table 2**). This finding suggests that *ZmWAK* deletion might have occurred after the domestication of maize from teosinte.

Moreover, we found that the inbred lines lacking *ZmWAK* usually had a common parent. For example, ten Chinese elite inbred lines without *ZmWAK* had the HZ4 genetic background (**Supplementary Table 3**). It appears that a lack of *ZmWAK* does not adversely affect agronomic performance and has been maintained in maize lines. Alternatively, as seen in the case of *RPM1* (ref. 42), the *ZmWAK* gene has a fitness cost, such that lack of *ZmWAK* can be retained and spread in maize germplasm, even when disease pressure is present.

We next sequenced the promoter and transcribed regions of *ZmWAK* from 23 teosinte and 54 maize lines, and we identified 61 haplotypes, the largest proportion of which were the Mo17 haplotype (**Supplementary Table 2**). There was no evidence for a selective sweep in the sequenced regions, except for exon 3, in which the ratio of nucleotide diversity in maize to that in teosinte was only 0.17—substantially lower than the corresponding ratio for other *ZmWAK* regions (0.37–1.32) (**Supplementary Fig. 8**). Exon 3 encodes the kinase domain and therefore might have evolved under functional constraints.

Interestingly, when we aligned the *ZmWAK* promoter regions, we found variable insertions at −462 bp relative to the start codon. Sequence analysis (based on the Genetic Information Research Institute database) indicated that these insertions originated from transposable element insertions (**Supplementary Fig. 9**), implying that pervasive transposable element activity once occurred at this location in the *ZmWAK* promoter, which might have been involved in shaping the functions of the different WAK family members[43].

DISCUSSION

Soil-borne *S. reilianum* teliospores invade maize during seed emergence and grow vegetatively to reach the flower primordial, where they cause head smut disease. In this study, we cloned the *ZmWAK* gene for quantitative resistance to maize head smut. Intriguingly, *ZmWAK*-mediated resistance occurs mainly in the mesocotyl of maize seedlings, rather than in the ear or tassel where typical symptoms occur. This resistance mode implies that *ZmWAK* has evolved to form a spatiotemporally optimized resistance strategy against maize head smut. Following its successful invasion of maize seedlings, *S. reilianum* develops biotrophic hyphae in the phloem of the mesocotyl and grows upwards along the phloem to invade the apical meristem. Concurrently, ZmWAK in xylem parenchyma cells and pericycle parenchyma cells, acting as a receptor-like kinase, might directly perceive the signals produced by the parasitic *S. reilianum* and trigger host defense responses to restrict pathogen growth and thereby reduce disease severity. In comparison to resistance-conferring *ZmWAK* alleles, *ZmWAK* alleles associated with susceptibility show decreased expression levels, remarkably in the mesocotyl but not in other tissues in seedlings. In brief, *ZmWAK*-mediated resistance occurs in the right place at the right time to achieve the most efficient disease control. Nevertheless, we cannot rule out the possibility that other tissues might be involved in the repression of mycelial growth, as *S. reilianum* has a long biotrophic life cycle that requires translocation to the ear or tassel to cause disease. With the availability of the *S. reilianum* genome[44], this plant pathosystem could serve as an excellent model to study the long-term interplay between host resistance gene(s) and biotrophic growth of a pathogen during the plant life cycle.

PAV is common in maize[39,40], and at least one PAV event has been associated with a quantitative trait[16]. The deletion of *ZmWAK* totally ablates expression of *ZmWAK* and imparts high susceptibility for maize to head smut. In addition, *ZmWAK* alleles vary considerably among maize germplasm, from null to susceptible and resistant alleles. *ZmWAK*-mediated quantitative resistance to head smut could mainly be attributable to the expression of *ZmWAK* in mesocotyl. Deletion

of *ZmWAK* in the HZ4 elite Chinese line did not result in any adverse effects, indicating that loss of *ZmWAK* can be tolerated and spread by the deployment of elite inbred lines. Finally, this characterization of *ZmWAK* will not only provide a model for subsequent resistance QTL cloning and characterization studies but will also greatly inform further hybrid breeding efforts to control head smut.

URLs. PROVEAN, http://provean.jcvi.org/index.php/; Genetic Information Research Institute database, http://www.girinst.org/; Food and Agriculture Organization (FAO) World Summit on Food Security, http://www.fao.org/wsfs/world-summit/en/; head smut (extended information) from the International Maize and Wheat Improvement Center (CIMMTY), http://maizedoctor.org/component/content/article/14-english/extended-information/512-head-smut-extended-information; ScanProsite, http://prosite.expasy.org/scanprosite/; MUSCLE, http://www.ebi.ac.uk/Tools/msa/muscle/.

METHODS

Methods and any associated references are available in the online version of the paper.

1. Wang, Z. *et al.* Research advance on head smut disease in maize. *J. Maize Sci.* **10**, 61–64 (2002).
2. Ghareeb, H., Becker, A., Iven, T., Feussner, I. & Schirawski, J. *Sporisorium reilianum* infection changes inflorescence and branching architectures of maize. *Plant Physiol.* **156**, 2037–2052 (2011).
3. Balint-Kurti, P.J. & Johal, G.S. in *Handbook of Maize: Its Biology* (eds. Bennetzen, H.L. & Hake, S.C.) 229–250 (Springer, 2009).
4. Johal, G.S. & Briggs, S.P. Reductase activity encoded by the *HM1* disease resistance gene in maize. *Science* **258**, 985–987 (1992).
5. Collins, N. *et al.* Molecular characterization of the maize *Rp1-D* rust resistance haplotype and its mutants. *Plant Cell* **11**, 1365–1376 (1999).
6. Zhao, B. *et al.* A maize resistance gene functions against bacterial streak disease in rice. *Proc. Natl. Acad. Sci. USA* **102**, 15383–15388 (2005).
7. Wisser, R.J., Balint-Kurti, P.J. & Nelson, R.J. The genetic architecture of disease resistance in maize: a synthesis of published studies. *Phytopathology* **96**, 120–129 (2006).

8. Richardson, K.L., Vales, M.I., Kling, J.G., Mundt, C.C. & Hayes, P.M. Pyramiding and dissecting disease resistance QTL to barley stripe rust. *Theor. Appl. Genet.* **113**, 485–495 (2006).
9. Miedaner, T. *et al.* Stacking quantitative trait loci (QTL) for *Fusarium* head blight resistance from non-adapted sources in an European elite spring wheat background and assessing their effects on deoxynivalenol (DON) content and disease severity. *Theor. Appl. Genet.* **112**, 562–569 (2006).
10. Parlevliet, J.E. Durability of resistance against fungal, bacterial and viral pathogens; present situation. *Euphytica* **124**, 147–156 (2002).
11. Krattinger, S.G. *et al.* A putative ABC transporter confers durable resistance to multiple fungal pathogens in wheat. *Science* **323**, 1360–1363 (2009).
12. Flint, J. & Mott, R. Finding the molecular basis of quantitative traits: successes and pitfalls. *Nat. Rev. Genet.* **2**, 437–445 (2001).
13. Remington, D.L., Ungerer, M.C. & Purugganan, M.D. Map-based cloning of quantitative trait loci: progress and prospects. *Genet. Res.* **78**, 213–218 (2001).
14. Yano, M. Genetic and molecular dissection of naturally occurring variation. *Curr. Opin. Plant Biol.* **4**, 130–135 (2001).
15. Holland, J.B. Genetic architecture of complex traits in plants. *Curr. Opin. Plant Biol.* **10**, 156–161 (2007).
16. Broglie, K.E. *et al.* Method for identifying maize plants with *RCG1* gene conferring resistance to colletotrichum infection. US patent 8,062,847 (2011).
17. Chen, Y. *et al.* Identification and fine-mapping of a major QTL conferring resistance against head smut in maize. *Theor. Appl. Genet.* **117**, 1241–1252 (2008).
18. Wang, M. *et al.* Genome-wide association study (GWAS) of resistance to head smut in maize. *Plant Sci.* **196**, 125–131 (2012).
19. Weng, J. *et al.* Molecular mapping of the major resistance quantitative trait locus *qHS2.09* with simple sequence repeat and single nucleotide polymorphism markers in maize. *Phytopathology* **102**, 692–699 (2012).
20. Zhao, X. *et al.* Marker-assisted introgression of *qHSR1* to improve maize resistance to head smut. *Mol. Breed.* **30**, 1077–1088 (2012).
21. Yang, Q., Zhang, D. & Xu, M. A sequential quantitative trait locus fine-mapping strategy using recombinant-derived progeny. *J. Integr. Plant Biol.* **54**, 228–237 (2012).
22. He, Z.H., He, D. & Kohorn, B.D. Requirement for the induced expression of a cell wall associated receptor kinase for survival during the pathogen response. *Plant J.* **14**, 55–63 (1998).
23. Diener, A.C. & Ausubel, F.M. *RESISTANCE TO FUSARIUM OXYSPORUM 1*, a dominant *Arabidopsis* disease-resistance gene, is not race specific. *Genetics* **171**, 305–321 (2005).
24. Sivaguru, M. *et al.* Aluminum-induced gene expression and protein localization of a cell wall–associated receptor kinase in *Arabidopsis*. *Plant Physiol.* **132**, 2256–2266 (2003).
25. He, Z.H., Cheeseman, I., He, D. & Kohorn, B.D. A cluster of five cell wall–associated receptor kinase genes, *Wak1–5*, are expressed in specific organs of *Arabidopsis*. *Plant Mol. Biol.* **39**, 1189–1196 (1999).
26. Lally, D., Ingmire, P., Tong, H.Y. & He, Z.H. Antisense expression of a cell wall–associated protein kinase, WAK4, inhibits cell elongation and alters morphology. *Plant Cell* **13**, 1317–1331 (2001).
27. Wagner, T.A. & Kohorn, B.D. Wall-associated kinases are expressed throughout plant development and are required for cell expansion. *Plant Cell* **13**, 303–318 (2001).
28. Zhang, S. *et al.* Evolutionary expansion, gene structure, and expression of the rice wall-associated kinase gene family. *Plant Physiol.* **139**, 1107–1124 (2005).
29. Liu, Y. *et al.* Isolation and characterisation of six putative wheat cell wall–associated kinases. *Funct. Plant Biol.* **33**, 811–821 (2006).
30. Dardick, C., Schwessinger, B. & Ronald, P. Non-arginine-aspartate (non-RD) kinases are associated with innate immune receptors that recognize conserved microbial signatures. *Curr. Opin. Plant Biol.* **15**, 358–366 (2012).
31. Brutus, A., Sicilia, F., Macone, A., Cervone, F. & De Lorenzo, G. A domain swap approach reveals a role of the plant wall-associated kinase 1 (WAK1) as a receptor of oligogalacturonides. *Proc. Natl. Acad. Sci. USA* **107**, 9452–9457 (2010).
32. Kohorn, B.D. *et al.* Pectin activation of MAP kinase and gene expression is WAK2 dependent. *Plant J.* **60**, 974–982 (2009).
33. Kohorn, B.D. *et al.* An *Arabidopsis* cell wall–associated kinase required for invertase activity and cell growth. *Plant J.* **46**, 307–316 (2006).
34. Martinez, C., Jauneau, A., Roux, C., Savy, C. & Dargent, R. Early infection of maize roots by *Sporisorium reilianum* f. sp. zeae. *Protoplasma* **213**, 83–92 (2000).
35. Fischer, G.W. & Holton, C.S. *Biology and Control of the Smut Fungi* (Ronald Press, 1957).
36. Balmer, D., Papajewski, D.V., Planchamp, C., Glauser, G. & Mauch-Mani, B. Induced resistance in maize is based on organ-specific defence responses. *Plant J.* **74**, 213–225 (2013).
37. Doehlemann, G. *et al.* Reprogramming a maize plant: transcriptional and metabolic changes induced by the fungal biotroph *Ustilago maydis*. *Plant J.* **56**, 181–195 (2008).
38. Buckler, E.S., Gaut, B.S. & McMullen, M.D. Molecular and functional diversity of maize. *Curr. Opin. Plant Biol.* **9**, 172–176 (2006).
39. Springer, N.M. *et al.* Maize inbreds exhibit high levels of copy number variation (CNV) and presence/absence variation (PAV) in genome content. *PLoS Genet.* **5**, e1000734 (2009).
40. Swanson-Wagner, R.A. *et al.* Pervasive gene content variation and copy number variation in maize and its undomesticated progenitor. *Genome Res.* **20**, 1689–1699 (2010).
41. Yang, X. *et al.* Characterization of a global germplasm collection and its potential utilization for analysis of complex quantitative traits in maize. *Mol. Breed.* **28**, 511–526 (2011).
42. Tian, D., Traw, M.B., Chen, J.Q., Kreitman, M. & Bergelson, J. Fitness costs of R-gene-mediated resistance in *Arabidopsis thaliana*. *Nature* **423**, 74–77 (2003).
43. Lisch, D. How important are transposons for plant evolution? *Nat. Rev. Genet.* **14**, 49–61 (2013).
44. Schirawski, J. *et al.* Pathogenicity determinants in smut fungi revealed by genome comparison. *Science* **330**, 1546–1548 (2010).

ONLINE METHODS

Plant materials. The maize inbred line Ji1037, derived from the Mo17 × (Mo17 × Suwan) backcross population, displays complete resistance to head smut. Suwan is a tropical maize germplasm from Thailand. We used anchored markers in the *qHSR1* region to amplify the region from both Ji1037 and its parental line, Mo17, and to sequence all PCR products. Sequence alignment of nine segments showed that the *qHSR1* region was identical for Ji1037 and Mo17, indicating that the region in Ji1037 originated from Mo17. HZ4 is an elite Chinese inbred line that is widely used in maize hybrid breeding but is highly susceptible to head smut. The F_1BC_1 and F_1BC_2 populations from the cross of Ji1037 and HZ4 were used to map *qHSR1*. Recombinants in the *qHSR1* region screened from various generations were backcrossed to HZ4 to develop F_1BC_3, F_2BC_2, F_1BC_4, F_2BC_3, F_1BC_6 and F_2BC_5 populations for the fine mapping of *qHSR1*. Here F_1 and F_2 indicate backcrossing started from the F_1 hybrid and an F_2 heterozygote, respectively. A collection of 62 diverse inbred lines, either highly susceptible (disease incidence of >40%) or resistant (disease incidence of <10%) to head smut, was used to test for an association between the candidate genes and head smut resistance. During the fine-mapping process, we developed a near-isogenic line, HZ4-*qHSR1*, for exploration of the molecular mechanism underlying *ZmWAK*-mediated resistance. HZ4-*qHSR1* contained the shortest *qHSR1*-spanning donor region (between STS1M3 and STS3M1) and had 96.3% genetic identity with HZ4 (as assessed with the Illumina MaizeSNP3K genotyping assay). In addition, we used a collection of 522 maize inbred lines and 184 teosinte accessions for an extensive survey of *ZmWAK* PAV, and 77 of these lines (23 teosinte and 54 maize; **Supplementary Table 2**) were subjected to sequencing of *ZmWAK*.

Field inoculation and phenotypic evaluation. Mapping populations and transgenic plants were planted at a seasonal growing location in Gongzhuling, Jilin Province, China, or in a winter nursery in Sanya, Hainan Province, China. Both locations were suitable for head smut infections to develop from artificial inoculation. Inoculums were collected from the galls of infected plants from the previous year and stored in a well-ventilated dark room. Seeds were sowed in seedling trays, covered with soil containing 0.1% teliospores and grown for 2 weeks; resulting seedlings were then transplanted to the field. Phenotypes were evaluated at the seed filling stage. Ears or tassels with smut or malformations were considered to be susceptible to head smut.

The progeny-test fine-mapping strategy. In each backcross generation, only recombinants within the mapped *qHSR1* region were selected for backcrossing to HZ4 to produce progeny for fine mapping. The progeny consisted of two genotypes in the *qHSR1* region—heterozygous Ji1037/HZ4 and homozygous HZ4/HZ4. We investigated each individual for its genotype and resistance performance and then calculated the mean resistance percentage for the two genotypes within recombinant-derived progeny. Paired *t* tests or χ^2 tests (used when a given genotype was represented by only a single recombinant) were used to test the significance of the difference between the two genotypes, with a significant (or non-significant) difference indicating the presence (or absence) of the Ji1037-derived *qHSR1* donor region. In other words, the parental recombinant was deduced to be resistant (or susceptible) to head smut. Comparison of the donor region to the deduced phenotype among multiple recombinants enabled us to narrow the *qHSR1* region. This mapping strategy, based on recombinant-derived progeny, effectively minimizes experimental errors resulting from genetic background noise and environmental variation[19].

Transgenic functional validation. The BAC clone Mo-J12 from a Mo17 BAC library was partially digested with Sau3AI, and digested fragments larger than 10 kb in size were purified and ligated into the BamHI-digested binary vector pCAMBIA1300 (Cambia). The *ZmWAK* marker SCAR6765 was used to screen for transgene-positive clones, which were then sequenced to confirm that they contained the intact and correct *ZmWAK* fragment. The construct used for transformation contained a 13.1-kb DNA fragment with the 6-kb gene, 3.9-kb promoter and 3.2-kb downstream regions, and it was designated as pCAMBIA1300-ZmWAK. The construct was transformed into the maize hybrid Hi-II with *Agrobacterium tumefaciens* EHA105. To produce the construct for RNAi, we amplified a 265-bp fragment from exon 3 of *ZmWAK* with a specific primer pair and cloned the PCR product into the pEasy-T1

vector (TransGen Biotech). The cloned fragment was cleaved with appropriate combinations of restriction enzymes for insertion into the RNAi vector pGreen-HY104 (ref. 45; provided by S. Yang (China Agricultural University)). The RNAi construct pGreen-WAK was introduced into Hi-II plants by bombardment into the callus. A progeny-test method similar to the one described above was adopted, where a χ^2 test of independence or a Fisher's exact test was used to determine whether the resistance was independent between transgenic and non-transgenic subgroups.

Laboratory inoculations with sporidia of *S. reilianum*. Inoculum was prepared as described by Ghareeb *et al.*[2]. Cell pellets were washed and resuspended in sterile double-distilled water to an absorbance of OD_{600} = 2.0. Ji1037 seeds were sterilized with 2% chloramine T (Sigma) for 15 min and were washed three times with sterile double-distilled water. Sterilized seeds were placed in germination boxes and grown on a 16-h light (28 °C): 8-h dark (25 °C) cycle at 60% relative humidity until the coleoptiles reached ~1–2 cm. Whole seedlings were soaked in mixed mating–type *S. reilianum* cultures at 25 °C at 50 rpm for 30 min for inoculation and then placed back in the germination boxes before tissue collection. Each sample contained tissue from at least five plants, and the mock-treated plants were inoculated with sterile double-distilled water.

Tissue sampling for determination of expression patterns. Ji1037 seeds were sterilized as described above and sowed in sterile soil under the same conditions used for seedling sampling. The coleoptile, root and mesocotyl were sampled at 3 DAS and stored at −80 °C, and the leaf was sampled at 7 DAS. For adult plant sampling, plants were grown in the field at the Shangzhuang Experimental Station in Beijing. Different tissues were sampled just before heading. Each sample contained tissue from at least five individuals.

RNA extraction and quantification. Total RNA was isolated from different maize tissues using TRIzol (Invitrogen) and treated with RNase-free DNase I to remove contaminating DNA. cDNA was synthesized using an M-MLV reverse transcriptase–based cDNA first-strand synthesis kit (Invitrogen). For semiquantitative PCR, 2.5 μg of RNA was reverse transcribed as the template for PCR (25 cycles of 95 °C for 30 s, 60 °C for 30 s and 72 °C for 15 s) with candidate gene–specific primers (*ZmWAK*, *ZmTIF*, *ZmHCH*, *ZmXa21-1* and *ZmXa21-2*). qPCR was performed using SYBR Green (Takara) with the Rotor-Gene Q 6000 cycler (Qiagen; 45 cycles of 95 °C for 10 s and 60 °C for 30 s, with signal acquisition at the end of each amplification cycle). *ZmTubulin1* was used as an internal control, and the $2^{-\Delta\Delta Ct}$ method was used to calculate relative gene expression. Each tissue contained three samples, and each sample was collected from at least five individuals. RNA expression for each sample was detected in three technical replicates.

RACE of *ZmWAK*. RACE was performed using the SMART RACE cDNA Amplification kit (Clontech). The 5′ RACE and 3′ RACE products were amplified using universal primer A mix paired with the *WAKGP2* and *WAKGP1* primers listed in **Supplementary Table 1**. The PCR products were subcloned into the pEasy-T1 vector and sequenced. The sequences of the 5′ and 3′ PCR products were aligned to obtain the full-length cDNA sequence for *ZmWAK*.

Phylogenetic analysis of WAK proteins. We downloaded all annotated maize WAK protein sequences from the NCBI database and selected only those having all three predicted functional domains (GUB, EGF_CA and kinase). The sequences of WAK proteins from several other plants were also included in the analysis, including AtWAK1 and AtWAK2 from *Arabidopsis*, OsWAK104 from rice, BdWAK4L from *Brachypodium distachyon*, Sb05g027230.1 from sorghum, SiWAK2L from *Setaria italica* and TRIUR3_01549_P1 from *Triticum urartu*. A phylogenetic tree was constructed using the maximum-likelihood method based on the JTT matrix-based model in MEGA 5.0. The classification of RD and non-RD kinases was performed with ScanProsite.

Subcellular localization of ZmWAK. The coding sequence of *ZmWAK* was amplified using the cDNA clone as the template. The PCR product was inserted into the pEZS-NL vector to create an ORF encoding an EGFP-fused protein

driven by the *35S* promoter. Maize protoplasts were isolated as described[46] and transformed with the *35S::WAK-EGFP* construct using the polyethylene glycol–mediated method. Transformed protoplasts were cultured at 28 °C in the dark overnight and observed under a confocal microscope (Zeiss). The *35S::WAK-EGFP* construct was also mixed with nanograde gold particles and bombarded into onion epidermal cells, which were then cultured at 28 °C in the dark for 8–10 h and observed under a confocal microscope (Nikon). Plasmolysis was induced by adding a 3% sucrose solution to the transformed onion epidermal cells.

Construction of the chimeric receptor and osmotic adjustment assays. The region encoding the cytoplasmic kinase domain of ZmWAK was amplified and ligated into the pEasy-T1 vector and used as the template for site-directed mutagenesis with the Easy Mutagenesis system (TransGen Biotech). The two active sites of the kinase domain, namely the ATP-binding site at Lys444 and the phosphorylation site at Ser640, were selected for mutagenesis. The chimeric BRI-ZmWAK receptor was constructed by combining the amplified coding regions for the cytoplasmic ZmWAK kinase domain and the ectodomain of BRI1 and inserting the chimeric construct into pEZS-NL to create an ORF encoding an EGFP fusion protein driven by the *35S* promoter. The same method was used to construct the two mutant chimeric receptors. The sequences of the primers used are listed in **Supplementary Table 1**. All of the constructs were introduced into protoplasts, and cells were treated with 2 µM epibrassinolide (Sigma) and then cultured at 28 °C in the dark for 36 h (ref. 30). The protoplast cells failing to tolerate high osmotic stress gradually shrink, resulting in the collapse of the plasma membrane and, finally, cell death. There are two states of dead cells: in one state, cells are already dead with cell debris and, in the other state, cells are shrunken and are in the process of dying. The numbers of intact and dead cells in the chimeric receptor– or empty vector–transformed and non-transformed (red auto-fluorescence) groups were counted under a fluorescence microscope.

Quantification of *S. reilianum* and *ZmWAK* in mesocotyl by quantitative PCR. HZ4 and HZ4-*qHSR1* seeds were sterilized as for the laboratory inoculations and placed at a depth of 3 cm in sterile soil containing 0.2% teliospores. Seeds were germinated and grown under a 16-h light (28 °C): 8-h dark (25 °C) cycle at 60% relative humidity. Mock-treated samples were sowed in sterile soil and grown under the same conditions. Samples were collected at 3 and 7 DAS from ≥10 individuals. A qPCR method comparing the expression of the *S. reilianum* actin gene (*sr11345*) to that of the maize tubulin1 gene (*ZmTubulin1*) was used to monitor the extent of fungal propagation[47]. Total RNA was isolated from the inoculated seedlings using TRIzol, and 3.5 µg was reverse transcribed to cDNA, which was then diluted 1:40 for qPCR. After 45 cycles of amplification, samples with sr11345 amplification curves below the stationary phase or with no PCR products were regarded as having undetectable levels. *ZmWAK* expression was assessed as described above for RNA extraction and quantification. The $2^{-\Delta\Delta Ct}$ method was used to calculate relative expression. Three biological replicates were analyzed, each with three technical replicates.

***In situ* hybridization.** Mesocotyl tissue was dissected from inoculated HZ4-*qHSR1* plants at 7 DAS. Tissues were fixed overnight in FAA solution (37% formaldehyde:glacial acetic acid:100% alcohol:DEPC-treated double-distilled water, 2:1:10:7 ratio), dehydrated in a graded ethanol series (50%, 70%, 85%, 95% and 100%) and then embedded in paraffin and sliced into 8-µm sections. RNA *in situ* hybridization was performed as described[48]. Probe primer sequences are listed in **Supplementary Table 1**, and probes were synthesized and labeled with digoxigenin by *in vitro* transcription using the T7 and SP6 RNA polymerases (New England BioLabs). The antisense probe was transcribed from the T7 promoter, and the sense probe was transcribed from the SP6 promoter. Images were acquired under the same photographic parameters.

Microscopy of *S. reilianum* in mesocotyl. Mesocotyl samples were dissected from inoculated HZ4-*qHSR1* plants at 7 DAS. Samples were sectioned by hand and stained with WGA–Alexa Fluor 488 as described[1]. Briefly, the mesocotyl was sectioned and soaked in 100% ethanol overnight, rinsed in double-distilled water three times and then incubated in 10% KOH overnight. After washes in double-distilled water, the sections were stained for 30 min in WGA–Alexa Fluor 488 solution in the dark (10 µg/ml in PBS, pH 7.4, and 0.02% Tween-20) and rinsed in water before observation under a confocal microscope (Zeiss).

PAV, diversity and neutrality detection. A pair of conservative primers was used to detect PAV at *ZmWAK* (SCAR6765) in 522 maize and 185 teosinte lines. Five primer pairs were designed to sequence the upstream, downstream and coding regions of *ZmWAK*. PCR products were subcloned into pEasy-T1, and three clones were picked for each PCR product for sequencing and alignment with MUSCLE, with manual adjustment using BioEdit software. Nucleotide diversity and Tajima's *D* statistic were calculated using DNaSP version 5.0.

45. Yu, H., Ito, T., Wellmer, F. & Meyerowitz, E.M. Repression of AGAMOUS-LIKE 24 is a crucial step in promoting flower development. *Nat. Genet.* **36**, 157–161 (2004).
46. Yoo, S.-D., Cho, Y.-H. & Sheen, J. *Arabidopsis* mesophyll protoplasts: a versatile cell system for transient gene expression analysis. *Nat. Protoc.* **2**, 1565–1572 (2007).
47. Marcel, S., Sawers, R., Oakeley, E., Angliker, H. & Paszkowski, U. Tissue-adapted invasion strategies of the rice blast fungus *Magnaporthe oryzae*. *Plant Cell* **22**, 3177–3187 (2010).
48. Zhang, X. *et al.* Laser microdissection of narrow sheath mutant maize uncovers novel gene expression in the shoot apical meristem. *PLoS Genet.* **3**, e101 (2007).